Infrasonic Detection of a Large Bolide over South Sulawesi, Indonesia on October 8, 2009: Preliminary Results

E. A. Silber • A. Le Pichon • P. G. Brown

Abstract In the morning hours of October 8, 2009, a bright object entered Earth's atmosphere over South Sulawesi, Indonesia. This bolide disintegrated above the ground, generating stratospheric infrasound returns that were detected by infrasonic stations of the global International Monitoring System (IMS) Network of the Comprehensive Nuclear-Test-Ban Treaty Organization (CTBTO) at distances up to 17 500 km. Here we present instrumental recordings and preliminary results of this extraordinary event. Using the infrasonic period-yield relations, originally derived for atmospheric nuclear detonations, we find the most probable source energy for this bolide to be 70 ± 20 kt TNT equivalent explosive yield. A unique aspect of this event is the fact that it was apparently detected by infrasound only. Global events of such magnitude are expected only once per decade and can be utilized to calibrate infrasonic location and propagation tools on a global scale, and to evaluate energy yield formula, and event timing.

Keywords infrasound · bolide · fireball · airburst · impact

1 Introduction

Medium sized Near Earth Objects (NEOs) (>10 m diameter) may penetrate deep into the atmosphere, though rarely, and cause significant damage on the ground (Chapman, 2008) and could potentially perturb regional climate trends (Toon et al. 1997). However, currently available models cannot accurately define the critical impactor size at which the regional climate is affected (Bland and Artemieva, 2003). A part of the problem is limited observational data, as records of significant NEOs are scarce. Therefore, various observational methods, including infrasound, are critical to re-evaluate airburst models and determine with more accuracy the size at which an object can influence the local climate.

Records of significant NEO impacts are rare. Klekociuk et al. (2005) and Arrowsmith et al. (2008) report multi-instrumental observations of two different impactors with energies of 20-30 kilotons of TNT (1 kT = 4.185×10^{12} J) occurring in the fall of 2004, while Brown et al. (2002) present infrasound data for two somewhat less energetic events over the Pacific in 2001. In all cases these events occurred over open ocean and much of the energetics information was compiled from records of the associated airwaves detected by infrasonic stations.

E. A. Silber (✉) • P. G. Brown
Department of Physics and Astronomy, University of Western Ontario, London, ON N6A 3K7, Canada. Phone:1-519-661-2111 x82385; Fax:1-519-661-2033; E-mail: elizabeth.silber@uwo.ca

A. Le Pinchon
CEA/DAM/DIF, F-91297 Arpajon, France

Infrasound is low frequency sound extending below the 20 Hz hearing threshold of the human ear and just above the natural oscillation frequency of the atmosphere (>0.01 Hz, Brunt-Väisälä frequency). It has the ability to propagate over long distances with very little attenuation, thus enabling the study of remote explosive sources (Hedlin et al., 2002). The International Monitoring System (IMS), operated by the Comprehensive Nuclear-Test-Ban Treaty Organization (CTBTO), features as one of its monitoring technologies, a global network of 42 fully certified infrasonic stations designed to detect nuclear explosions (CTBTO web: http://www.ctbto.org).

Bright meteors (also known as fireballs) fall into the category of events that can be detected and consequently studied using infrasound (ReVelle, 1976, 1997; Brown et al., 2002a). Fireballs are produced by large meteoroids which may penetrate deep into the atmosphere and generate a cylindrical blast wave during their hypersonic passage, which decays to low frequency infrasonic waves that propagate over great distances (ReVelle, 1976; Edwards, 2010; Le Pichon et al., 2002a, Brown et al., 2002; Brown et al., 2003). Global impacts detected infrasonically can provide a valuable tool in the estimation and validation of the influx rate of meter sized and larger meteoroids (Brown et al. 2002; Silber et al. 2009). Very often, infrasound offers the only available record when it comes to major impacts over open ocean. Infrasound observations can provide crucial trajectory and energetics information for interesting events which otherwise lack such information (e.g. the Carancas crater forming impact in Peru in 2007 (Brown et al., 2008; Le Pichon et al., 2008)). Here we present evidence that a significant NEO impact occurred on October 8, 2009 over South Sulawesi, Indonesia based primarily on infrasonic recordings of the blast wave detected across the globe; this may have been one of the most energetic impactors to collide with the Earth in recent history.

2 The Indonesian Bolide

At 2:57 UTC (10:57 a.m. local time) on October 8, 2009 a loud rumbling sound and ground shaking startled the people of the town of Bone, South Sulawesi, Indonesia (4.5ºS, 120ºE). Eyewitnesses who ran out their homes in fright saw a very bright object flying across the sky, subsequently disintegrating in the mid air, leaving a thick dusty smoke trail behind (Surya news report, in Indonesian: http://www.surya.co.id/2009/10/09/ledakan-misterius-guncang-sulsel.html). A news article stated that there are reports from local residents that the surviving remnants of the object may have crashed into the sea (Surya news report, in Indonesian: http://www.surya.co.id/2009/10/09/leda kan-misterius-guncang-sulsel.html).

Shortly thereafter, the national media, including Metro TV of Jakarta and two news agencies, The Jakarta Globe and The Jakarta Post, released a number of reports, including an amateur video of the smoke trail (Figure 1). Features and the appearance of the smoke trail are consistent with dust trails of other fireballs observed in a similar manner (e.g. the Tagish Lake fireball (Hilderbrand et al, 2006)), indicating a probable meteoritic origin of the event. As per The Jakarta Globe, the airburst caused damage to several houses in Panyula village (The Jakarta Globe, available at: http:// www.thejakartaglobe.com/home/astronomer-sulawesi-blast-bigger-than-atom-bomb-and-caused-by-met eorite/338073) and the police department in Bone was flooded with reports of audible sounds extending as far as 11 km from Latteko, Bone district, South Sulawesi (The Jakarta Globe: available at: http://thejakartaglobe.com/home/mysterious-explosion-panics-locals-in-south-sulawesi-police-still-investigating/334246). Unfortunately, there was one casualty, a 9 year old girl with an underlying heart condition who went into cardiac arrest upon hearing the thunderous sounds (The Jakarta Globe, available at: http://www.thejakartaglobe.com/home/astronomer-sulawesi-blast-bigger-than-atom-bomb-

and-caused-by-meteorite/338073). Initially, local people speculated that the event was caused by a falling airplane; however, South Sulawesi Police spokesman Sr. Comr. Hery Subiansauri confirmed that no aircraft was involved nor any other air incident had occurred. The extraterrestrial nature of the event was confirmed by Thomas Djamaluddin, head of the Lapan Center for Climate and Atmosphere Science (The Jakarta Post, available at: http://www.thejakartapost.com/news/2009/10/08/blast-may-be-result-falling-space-waste-or-meteorite-lapan.html).

Upon scrutinizing scrutinizing these reports, we undertook a thorough investigation of infrasonic records of all IMS infrasound stations to search for possible signals from the air explosion.

Figure 1. A screenshot from Metro TV news report showing an amateur video of the smoke trail, twisted by the wind (You Tube, available at: http://www.youtube.com/watch?v=yeQBzTkJNhs&videos=jkRJgbXY-90).

3 Data Processing and Analysis

We were able to examine a total 31 infrasound stations in the IMS network which were providing data at the time of the event. Probable signals originating from 4.5°S, 120°E were detected at 17 IMS stations (Figure 2), which we correlated with the event. Table 1 summarizes data from all stations which detected the signal, sorted by distance. The signal was extraordinary in two aspects: first, it was detected by many infrasound stations, some of which are at extreme distances (>17,000 km), and second, that most of the signal energy is contained in very low frequencies, indicative of a source yielding very high energy. Infrasonic signals were analyzed using two independent methods, Matseis 1.7 (Harris and Young, 1997; Young et al., 2002) and Progressive Multi-Channel Correlation Method (PMCC) (Cansi, 1995).

First, infrasound data across each station have been array processed in windows (typically of 30-60 second length) to search for coherent signals with consistent back-azimuth measurements for several adjacent windows using the analysis package Matseis 1.7 (Harris and Young, 1997; Young et al., 2002). To determine the arrival azimuth for a coherent signal, we used the standard method of cross-correlating the output between each sensor of an array and performed beamforming of the signals across the array

Figure 2. A global map (courtesy of CTBTO, web: http://www.ctbto.org) showing all stations (black circles) that detected the Indonesian bolide event circled in red.

Table 1. Summary of all detections, sorted by distance. We include results for two methods of signal detection (MatSeis and PMCC).

Distance (km)	Station ID	Latitude (deg)	Longitude (deg)	True Back Azimuth (deg)	Observed Back Azimuth (deg)	Arrival time	Signal Duration (s)	Minimum Celerity (m/s)	Maximum Celerity (m/s)	Peak-to-peak Amplitude via PMCC (Pa)	Peak-to-peak Amplitude via MatSeis (Pa)	Period at max Amplitude via PMCC (s)	Period at max PSD via MatSeis (s)	Period at max Amplitude via MatSeis (s)
2099	I39PW	7.5	134.5	230	264	04 :39 :51	1235	283	340	...	1.57	...	13.65	14.87
2291	I07AU	-19.9	134.3	316	318	04 :55 :46	850	287	320	2.823	3.091	6.96	7.88	5.79
3350	I04AU	-34.6	116.4	7	9	05 :59 :18	1370	271	305	0.471	0.526	5.36	7.31	7.11
4920	I30JP	35.3	140.3	210	211	07 :33 :43	1280	280	302	0.642	0.6077	25.60	7.88	7.89
5009	I05AU	-42.5	147.7	319	319	07 :37 :01	690	280	292	0.542	0.874	10.50	29.26	25.23
5386	I22FR	-22.2	166.8	284	285	07 :45 :08	1340	290	312	0.165	0.127	5.30	20.48	21.07
5543	I45RU	44.2	132.0	196	197	08 :04 :54	1450	278	300	1.192	1.1873	10.70	17.07	19.79
7296	I46RU	53.9	84.8	222	224	09 :46 :19	1490	281	298	0.803	...	15.20	...	...
7323	I44RU	53.1	157.7	141	141	09 :49 :46	2450	268	294	0.363	0.7896	6.99	18.62	18.29
8577	I55US	-77.7	167.6	311	305	10 :55 :07	1060	289	299	0.168	0.145	12.10	17.07	17.62
10573	I53US	64.9	-147.9	270	270	12 :49 :47	830	291	297	0.488	0.418	12.70	12.80	14.66
11594	I26DE	48.8	13.7	80	80	14 :28 :51	185	278	279	0.04	...	5.48	...	...
11900	I18DK	6.7	-4.9	350	340	14 :15 :26	1100	284	292	0.693	0.645	18.10	25.60	21.81
12767	I56US	48.3	-117.1	293	322	14 :54 :45	1520	286	292	0.765	0.764	14.70	13.65	11.83
13636	I13CL	15.3	-23.2	244	240	16 :26 :53	1310	273	281	0.618	0.606	12.10	11.38	11.31
13926	I17CI	-33.7	-78.8	91	87	17 :05 :34	615	270	274	0.128	0.1347	12.10	9.31	8.64
17509	I08BO	-16.2	-68.5	203	218	18 :54 :45	30	...	305	...	0.933	...	17.07	16.34

(Evers and Haak, 2001). A sample output is shown in Figure 3. In total 15 positive detections were identified in this way, using the approximate location and timing from media reports and expected typical stratospheric propagation speeds as a guide to isolate the period of most probable signal arrival on each array. This procedure was repeated for multiple bandpasses to try and isolate any coherent signal from the station noise.

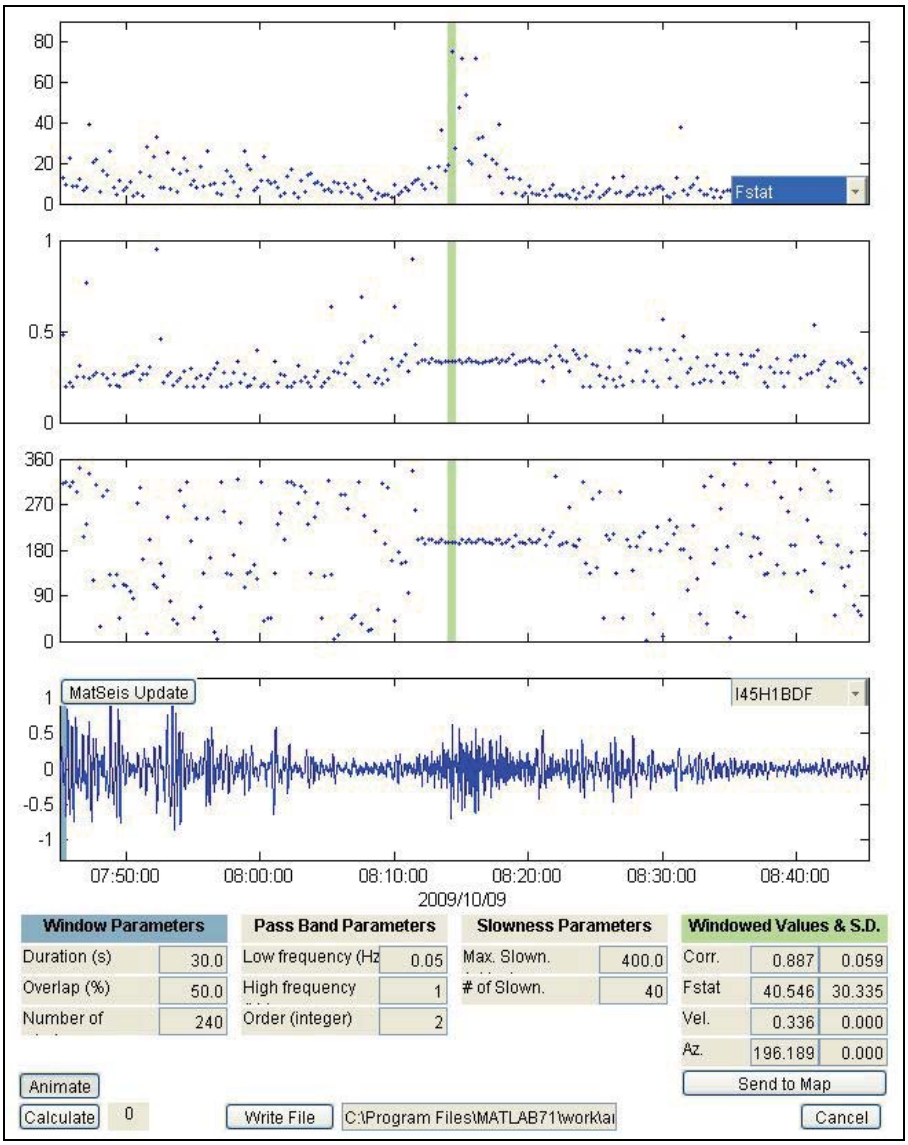

Figure 3. An example of signal observed at I45RU, located 5543 km from the source. The top window is the F-statistic, a measure of the relative coherency of the signal across the array elements in any particular window, the second window represents the apparent trace velocity of the acoustic signal across the array in the direction of the peak F-stat, while the third window shows the best estimate for the signal back-azimuth in the direction of maximum F-stat for each window. The fourth window shows the bandpassed raw pressure signal for one array element.

The second method, PMCC, for analysing the data, sensitive to coherent signals with very low signal-to-noise ratio (SNR), yielded positive detections at a total of 16 IMS stations. This technique has been successfully implemented in detections of other bolides (cf. Arrowsmith et al., 2008), as it searches for coherent signals in both frequency and time windows, selecting detections of similar parameters to identify coherent signals (Brachet et al., 2010) (Figure 4).

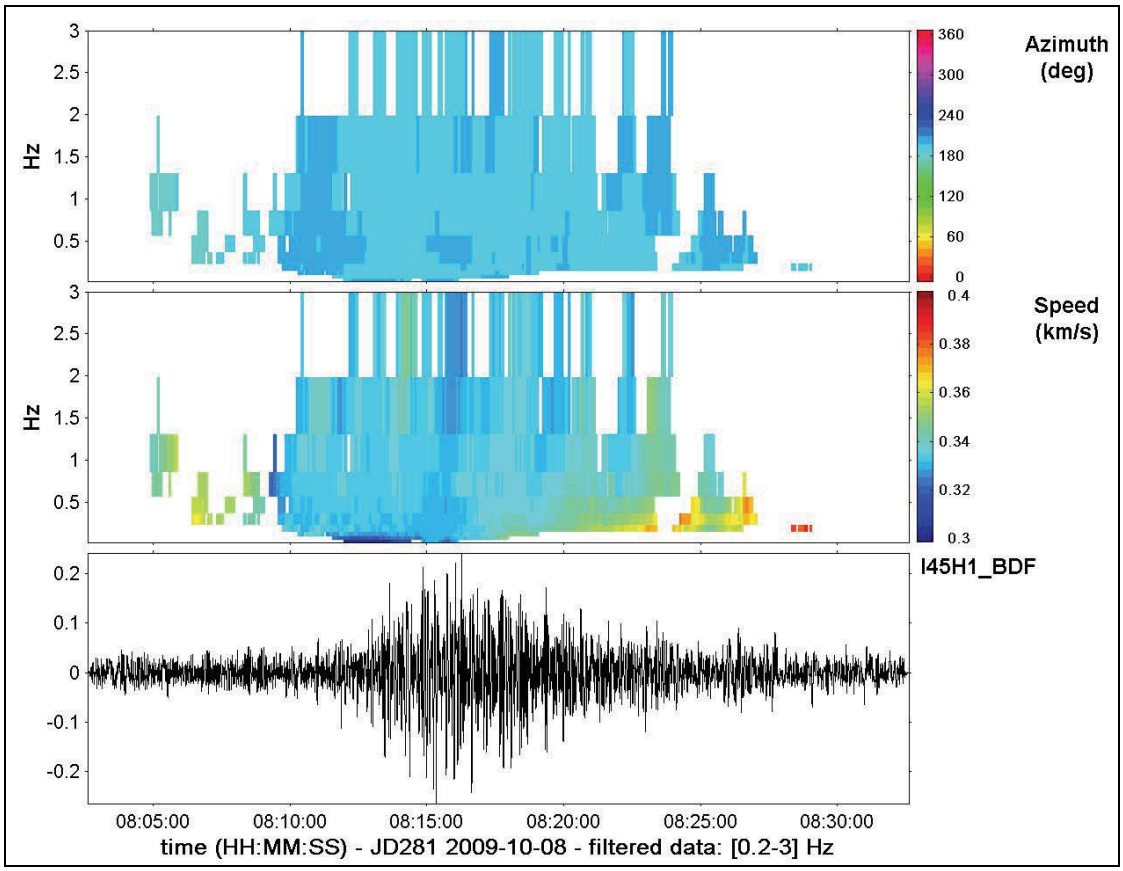

Figure 4. Results from array processing using the PMCC algorithm for the IMS station I45RU. The top window gives the observed azimuth, while the middle window represents the trace velocity of the signal. The bottom window shows the bandpassed raw pressure signal for one array element.

We have also established a geolocation using the nine closest stations (Figure 5) by utilizing a non-linear system of equations describing the propagation of the detection waves through the atmosphere, where the inverse location algorithm is based on Geiger's approach (1910). The location results are obtained assuming a homogeneous half-space with a typical celerity value of 290 m/s for each individual phase without azimuthal correction (Brown et al., 2002). In order to determine the location errors, the 95% confidence ellipses are estimated by repeatedly running the linearized least-squares inversion with arbitrary sub-sets of the input data within ±10° and ±30 m/s ranges of uncertainties for the azimuths and celerity, respectively.

The maximum peak-to-peak amplitude was determined by bandpassing the stacked, raw waveform using a second-order Butterworth filter and then applying the Hilbert Transform (Dziewonski and Hales, 1972) to obtain the peak of the envelope. The filter cutoff frequencies were typically 0.05 Hz for the low frequency and up to 2.1 Hz for the high frequency (with few exceptions) and were

determined using a power spectral density (PSD) method where the signal segment of the waveform was superimposed over the average of the prior and post background noise (of equal length), all being divided into equal windows (50-170 seconds in length, depending on station), establishing a frequency band which lies above the noise. Therefore, the low and high frequency cutoffs would be selected where the signal rises above the noise on the low end or descends into the noise on the high end of the spectrum, respectively.

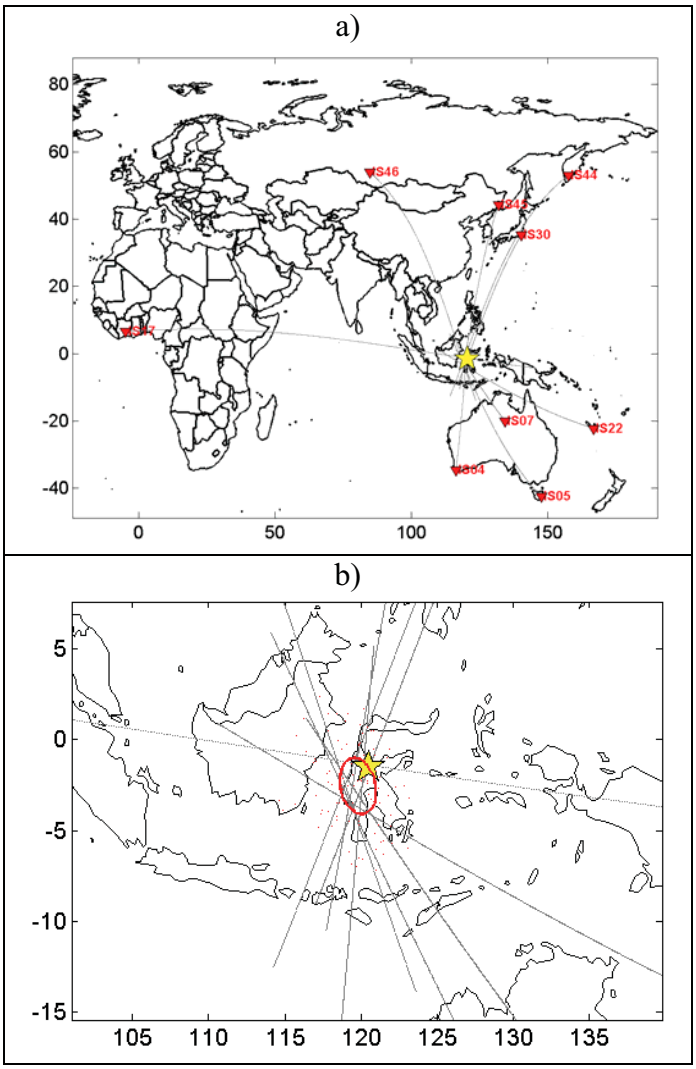

Figure 5. Map showing the geolocation. The best fit solution was obtained using nine stations closest to the Indonesian bolide event.

To measure the dominant period at maximum peak-to-peak amplitude, two independent techniques were employed. First, the dominant period at maximum frequency was acquired from the residual power spectral density (PSD) obtained using the method described above, except the noise PSD was subtracted from the signal PSD. The inverse of the frequency at maximum residual PSD was used to obtain the dominant period. Second, the period at maximum peak-to-peak amplitude was tabulated by

measuring the zero crossings of the stacked waveform at each station (cf. ReVelle, 1997) in the same bandpass. The periods obtained using these two techniques show a very strong 1:1 correlation (Figure 6), indicating that this methodology is robust in itself.

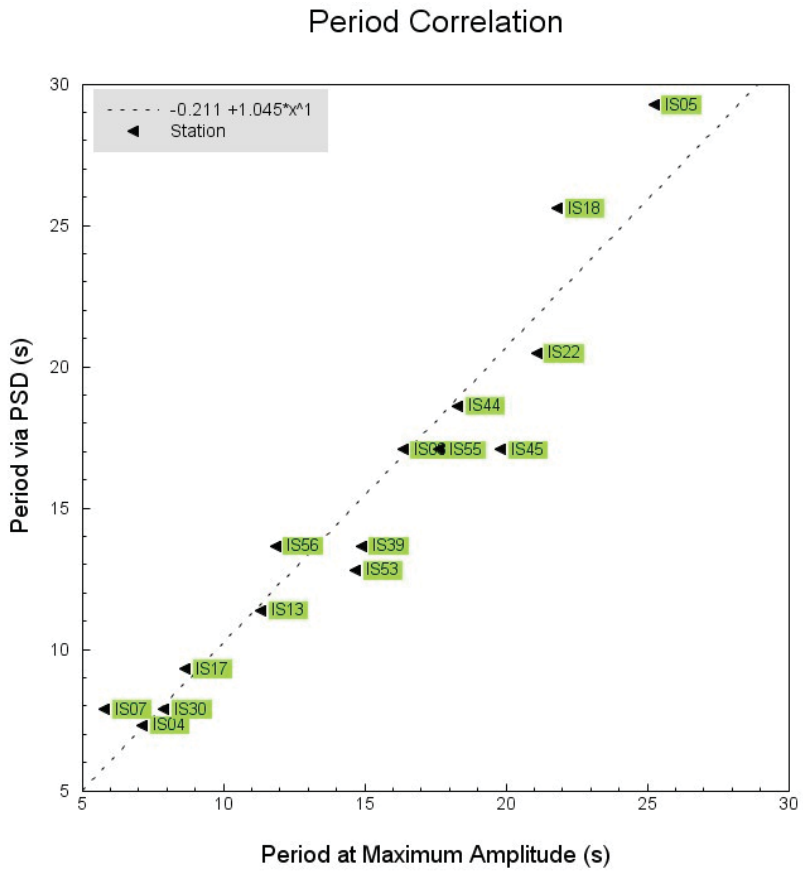

Figure 6. The dominant period correlation using two methods: PSD (vertical axis) and zero-crossings (horizontal axis).

4 Estimating the Source Energy

There are several empirical relations, relying on either the period at maximum amplitude or range and signal amplitude, which can be utilized in estimating source energy from infrasound measurements (Edwards et al., 2006). The yield estimates based on infrasonic amplitude are very uncertain in this instance as the propagation distances are much larger than is typical and outside the range limits where such relations have been developed (Edwards et al, 2006). In general, infrasonic period is less modified during propagation than amplitude (cf. Mutschlecner et al., 1999; ReVelle 1997; ReVelle 1974) and thus the period relationship is expected to be more robust. The Air Force Technical Application Centre (AFTAC) period-yield relations which are commonly used for large atmospheric explosions, are given by ReVelle [1997], as:

$$\log(E/2) = 3.34\log(P) - 2.58 \qquad E/2 \le 100kt \qquad (1)$$

$$\log(E/2) = 4.14\log(P) - 3.61 \qquad E/2 \ge 40kt \qquad (2)$$

Here, E is the total energy of the event (in kilotons of TNT), P is the period (in seconds) at maximum amplitude of the waveform. Since these relations were originally derived from nuclear explosions, the factor ½ must be incorporated in order to account for energy loss due to radiation for low altitude nuclear airbursts (Glasstone and Dolan, 1977). Even though there are a number of effects that may adversely influence and change the period at maximum amplitude during long range propagation of infrasound, this approach remains more robust than the maximum amplitude based relations, since it shows better agreement with energy estimates for bolide events which had their energies estimated by other methods (Silber et al, 2009; Brown et al., 2002).

5 Results and Discussion

There are total of 17 detections, 16 obtained with PMCC and 15 obtained with MatSeis (Table 1). These detections overlap, except for the signal detected via MatSeis at the Bolivian station (I08BO), 17 509 km from the source. This signal, though very weak and short in duration (~30 seconds) compared to other signals (>185 seconds), shows a strong correlation to the bolide. The correlation indicators are the arrival time, the signal velocity, the dominant period and the apparent agreement between the observed and expected azimuth. The first arrival was detected almost two hours after the event at the closest IMS station, I39PW, at 04:39:51 UTC, while it took nearly 15 hours for the last bits of the signal to arrive to I08BO. Duration of the signal at each station (not including I08BO) was quite significant, ranging from 3 minutes up to 41 minutes. All infrasound signals from the event show similar characteristics, such as long period and very low frequency content, consistent with a large blast radius and consequently a large energy source (ReVelle, 1976). Furthermore, average signal celerities are between 270 m/s and 320 m/s, indicative of stratospheric duct signal returns.

The presence of high altitude winds affects the propagation of the signal in such way that it amplifies the downwind propagation, while it attenuates upwind propagation (c.f. Mutschlecner and Whitaker, 2010; Davidson and Whitaker, 1992; Reed 1969a). Most of the detecting stations are located east from the source and in October the stratospheric winds are predominantly westerly in the northern hemisphere (Webb, 1966). Average signal celerities (defined by the ratio between the horizontal propagation range and the travel time) are between 0.27 and 0.32 km/s, which is consistent with stratospheric duct signal returns. We also searched for possible antipodal signals, but found none.

The geolocation ellipse (Figure 5), computed using azimuths and arrival times, points to 4.9°S and 122.0°E with mean residuals of 2.9°. The source time estimated from this location is 02:52:22 with a residual of 1320 s. The accuracy of the source location strongly depends on the atmospheric wind and temperature profiles at the place and time of the event.

To establish the best possible energy estimate of the Indonesian bolide, the average global period as well as individual periods, using both previously described zero-crossings and PSD methods, for each station were utilized. Table 2 shows the summary of energy estimates. The combined average periods of all phase-aligned stacked waveforms at each station produce a global average of 14.8 seconds (zero crossings method) and 15.3 seconds (PSD method), corresponding to a mean source energy of 42.7 kt of TNT and 47.3 kt of TNT, respectively. Using the measurements from nine stations with the highest signal-to-noise ratio energy yield is 66.1 kt of TNT (zero crossings method) and 78.1 kt of TNT (PSD

method). The standard deviation of energy measurements across all stations is approaching the measurement itself, but this is expected because the signal usually emanates from different portions of the bolide trail as observed at different stations. Our best source energy estimate is 70 ± 20 kt TNT, with the error bounds representing the spread in the average from the different approaches (Table 2).

Table 2. List of all detecting stations and their periods measured via two methods (zero-crossings at maximum amplitude in time domain and frequency at maximum PSD in frequency domain), as well as energy measurements for each station, where appropriate AFTAC relations were used (equation (1) or equation (2)).

Energy estimate as a function of period					*Energy estimate as a function of SNR*				
Station ID	Period via zero crossings (s)	Energy (kt of TNT)	Period via PSD (s)	Energy (kt of TNT)	Station ID	Period via zero crossings (s)	Energy (kt of TNT)	Period via PSD (s)	Energy (kt of TNT)
IS04	7.11	3.68	7.31	4.05	IS04	7.11	3.68	7.31	4.05
IS05	25.23	312.64	29.26	577.07	IS05	25.23	312.58	29.26	577.07
IS07	5.79	1.85	7.88	5.19	IS07	5.79	1.86	7.88	5.19
IS08	16.34	59.33	17.07	68.61	IS18	21.81	155.65	25.60	332.00
IS13	11.31	17.37	11.38	17.71	IS44	18.29	86.46	18.62	91.75
IS17	8.64	7.06	9.31	9.06	IS45	19.79	112.50	17.07	68.61
IS18	21.81	155.69	25.60	332.00	IS53	14.66	41.30	12.80	26.25
IS22	21.07	138.75	20.48	126.15	IS55	17.62	76.33	17.07	68.61
IS30	7.89	5.22	7.88	5.19	IS56	11.83	20.17	13.65	32.56
IS39	14.87	43.30	13.65	32.56	Average E (kt of TNT)		**90.06**		**134.01**
IS44	18.29	86.42	18.62	91.75					
IS45	19.79	112.45	17.07	68.61	*Energy estimate as a function of SNR (period average)*				
IS53	14.66	41.25	12.80	26.25	Total	16.88	**66.10**	14.46	**78.11**
IS55	17.62	76.29	17.07	68.61					
IS56	11.83	20.19	13.65	32.56					
Average E (kt of TNT)		**72.10**		**97.69**					
Energy estimate based on averaged global period									
Total	14.81	**42.73**	15.27	**47.30**					

6 Conclusions

The Indonesian bolide of 8 October, 2009, detected infrasonically on a global scale, was perhaps the most energetic event since the bolide of 1 February, 1994 (McCord et al., 1995) and may have exceeded it in total energy. We have no other instrumental records of this event other than casual video records of the dust trail emphasizing again the value of infrasonic monitoring of atmospheric explosive sources. Low frequency waves were observed at 17 IMS stations of the CTBTO network, making it one of the best infrasonically documented events (DTRA Verification Database, available at: http://www.rdss.info).

Using an average impact velocity for Near Earth Objects (NEO) of 20.3 km/s, the energy limits (50-90 kt of TNT) suggested by this analysis correspond to an object 8-10 m in diameter. Given our upper limit in energy and a lowest possible entry velocity of 11.2 km/s, the upper limit to the mass for this meteoroid is < 6000 tonnes. Based on the flux rate from Silber et al. (2009), such objects are

expected to impact the Earth on average every 10-22 years. Additional instrumental records of this unique event would prove valuable in understanding in more detail its interaction with the atmosphere and documenting possible local atmospheric perturbations.

Additional instrumental records of this exceptional event, such as seismic, ground video recordings, satellite and possible meteorites, would prove valuable in understanding such occurrences and documenting possible local atmospheric perturbations. Since events like this one are rather rare, it is essential to maximize all aspects of such observations in order to validate propagation models at global scale, implement and better understand the spatial and temporal influences of atmospheric dynamics over propagation times, especially over long distances, and to evaluate energy yield formula and establish what information, not available via other techniques, can be derived from infrasonic measurements.

Acknowledgements

EAS and PGB thank the Natural Sciences and Engineering Research Council of Canada and Natural Resources Canada, and express their gratitude to the Meteoroid Environment Office of the National Aeronautics and Space Administration for funding the Meteoroids 2010 conference.

References

S.J. Arrowsmith, D.O. Revelle, W. Edwards, P. Brown, Earth Moon Planets (2008) doi: 10.1007/s11038-007-9205-z

N.A. Artemieva, P.A. Bland, P.A. Meteorit. Planet. Sci. 38 (2003)

N. Brachet, D. Brown, R. Le Bras, P. Mialle, J. Coyne, in Infrasound Monitoring for Atmospheric Studies (Springer Netherlands, 2010) pp. 77-118

P. Brown, D.O. ReVelle, E.A. Silber, W.N. Edwards, S. Arrowsmith, L.E. Jackson, G. Tancredi, D. Eaton, J. Geophys. Res.-Planet (2008) doi:10.1029/2008JE003105

D. Brown, C.N. Katz, R. Le Bras, M.P. Flanagan, J. Wang A.K. Gault, Pure. Appl. Geophys. (2002) doi: 10.1007/s00024-002-8674-2

P. Brown, R.E. Spalding, D.O. ReVelle, E. Tagliaferri, S.P. Worden, Nature. (2002a) doi: 10.1038/nature01238

P.G. Brown, P. Kalenda, D.O. ReVelle, J. Borovicka, Meteorit. Planet. Sci. (2003) doi: 10.1111/j.1945-5100.2003.tb00296.x

P.G. Brown, R.W. Whitaker, D.O. ReVelle, E. Tagliaferri, Geophys. Res. Lett. (2002) doi: 10.1029/2001GL013778

Y. Cansi, Geophys. Res. Lett. (1995) doi: 10.1029/95GL00468

C.R. Chapman, Earth Moon Planet (2008) doi:10.1007/s11038-007-9219-6

M. Davidson, R.W. Whitaker, Los Alamos National Laboratory Report LA-12074-MS (1992)

A. Dziewonski, A. Hales, in Methods in Computational Physics (Academic Press, New York, 1972), pp. 39–84

W. Edwards, in Infrasound Monitoring for Atmospheric Studies (Springer Netherlands, 2010), pp. 361-414

W. N. Edwards, P.G. Brown, D. O. ReVelle Estimates of meteoroid kinetic energies from observations of infrasonic airwaves, Journal of Atmospheric and Solar-Terrestrial Physics (2006) doi: 10.1016/j.jastp.2006.02.010

L.G. Evers, H.W. Haak, Geophys. Res. Lett. (2001) doi: 10.1029/2000GL011859

L.Geiger, K. Ges. Wiss. Gött. 4, 331-349 (1910)

S. Glasstone, P.J. Dolan, in The Effects of Nuclear Weapons (United States Department of Defence and Department of Energy, Washington, DC, USA, 1977)

J.M. Harris, C.J. Young, Seismol. Res. Lett. 68, 307–308 (1997)

M. Hedlin, M. Garćes, H. Bass, C. Hayward, E. Herrin, J. Olson, C. Wilson, EOS (2002) doi: 10.1029/2002EO000383

A.R. Hildebrand, P.J.A. McCausland, P.G. Brown, F.J. Longstaffe, S.D.J. Russell, E. Tagliaferri, J.F. Wacker, M.J. Mazur, Meteorit. Planet. Sci. (2006) doi: 10.1111/j.1945-5100.2006.tb00471.x

A. Le Pichon, J.M. Guérin, E. Blanc, D.J. Raymond, Geophys. Res. Lett. (2002a) doi:1029/2001JD001283

A. Le Pichon, K. Antier, Y. Cansi, B. Hernandez, E. Minaya, B. Burgoa, D. Drob, L.G. Evers, J. Vaubaillon, Meteorit. Planet. Sci. (2008) doi: 10.1111/j.1945-5100.2008.tb00644.x

A.R. Klekociuk, P.G. Brown, D.W. Pack, D.O. ReVelle, W.N. Edwards, R.E. Spalding, E. Tagliaferri, B.B. Yoo, J. Zagari Nature (2005) doi: 10.1038/nature03881
T.B. McCord, J. Morris, D. Persing, E. Tagliaferri, C. Jacobs, R. Spalding, L. Grady, R. Schmidt, J. Geophys. Res. (1995) doi: 0148-0227/95/94JE-0280250
J.P. Mutschlecner, R.W. Whitaker, in Infrasound Monitoring for Atmospheric Studies (Springer Netherlands, 2010), p. 455-474
J.P. Mutschlecner, R.W. Whitaker, L.H. Auer, Los Alamos National Laboratory Technical Report, LA-13620-MS (1999)
J.W. Reed, Sandia Laboratories report SC-RR-69-572 (1969a)
D.O. ReVelle, in Annals of the New York Academy of Sciences, ed. by J.L. Remo (New York Academy of Sciences, 1997), p. 822
D. O. ReVelle, J. Geophys. Res. (1976) doi: 10.1029/JA081i007p01217
D.O. ReVelle, Acoustics of Meteors, PhD Dissertation, University of Michigan, 1974
E.A. Silber, D.O. ReVelle, P.G. Brown, W.N. Edwards, J. Geophys. Res.-Planet (2009) doi: 10.1029/2009JE003334
O.B. Toon, K. Zahnle, D. Morrison, R.P. Turco, C. Covey, Rev. Geophys. (1997) doi: 10.1029/96RG03038
W.L. Webb, Structure of the Stratosphere and Mesosphere (Academic Press, New York, 1966)
C.J. Young, E.P. Chael, B.J. Merchant, Proceedings of the 24th Seismic Research Review (2002)